RESEARCH

Aging Pathobiology and Therapeutics 2023; 5(2): 59-65 *59*
DOI: 10.31491/APT.2023.06.113

Targeted regulation of senescence-associated secretory phenotype with an aptamer-conjugated activatable senomorphic

Yuqi Xie[a, #], Jili Li[a, #], Pingyu Wu[a], Linlin Wang[a], Donghui Hong[a], Jian Wang[a], Yanlan Liu[a, *]

[a] *Molecular Science and Biomedicine Laboratory (MBL), State Key Laboratory of Chemo/Biosensing and Chemometrics, College of Chemistry and Chemical Engineering, Aptamer Engineering Center of Hunan Province, Hunan University, Changsha, Hunan 410082, China.*

This article belongs to the Special Issue: Research advances on cellular senescence and cancer

Abstract

Background: Senomorphics have been considered as an effective alternative paradigm of senotherapeutics to regulate cellular senescence and related disorders by inhibiting the deleterious effects of senescence-associated secretory phenotype (SASP) components secreted by senescent cells without inducing cell death. However, current senomorphic drugs usually exhibit low selectivity towards senescent cells and inevitably cause unwanted side effects, highlighting the need to develop innovative senomorphic strategies for the specific regulation of cellular senescence.

Materials and methods: To address this challenge, here we design a novel class of senomorphics with active cell targeting and activatable activities for selective regulation of SASP by conjugating a senescent cell-targeted aptamer with a SA-β-gal-activated H_2S donor. Using senescent BJ cells as a cell model, a series of investigations were performed to evaluate the performance of the engineered senomorphic (Apt-H_2SD) for cell-specific regulation of SASP during cellular senescence.

Results: Apt-H_2SD demonstrated specific binding and accumulation to senescent cells over proliferating cells through the aptamer-mediated cell targeting. Upon internalization, Apt-H_2SD was efficiently activated by the accumulated SA-β-gal in senescent cells, leading to the release of H_2S precursor and subsequently suppressing the expression of three important SASP factors (IL-6, IL-1β and MMP3) at the mRNA level.

Conclusion: Our results strongly support the potential of Apt-H_2SD as a valuable senomorphic. With rational design of the molecular structure, this study may provide a general strategy to construct advanced senescence-targeted activatable senomorphics for precise intervention of cellular senescence and age-related diseases.

Keywords: Senescence-associated secretory phenotype, senomorphics, L1CAM, cellular senescence

Introduction

The senescence-associated secretory phenotype (SASP), as one of the major metabolic and signaling characteristics of senescent cells, has long been a hot topic in the field of senescence and aging research [1, 2]. SASP can accelerate senescence in an autocrine manner and induce senescence of surrounding cells in a paracrine manner, cumulatively exacerbating the development of age-related diseases such as cancer, cardiovascular diseases, and neurodegenerative disorders [3, 4]. Thus, suppression of SASP has been considered an effective way to treat and/or prevent age-related diseases [5]. In this context, the development of drugs capable of specifically regulating SASP has become a research frontier in both academic and clinical fields.

Of particular importance are senomorphics, a class of senotherapeutics capable of maintaining the metabolic homeostasis and controlling pathological progression by attenuating SASP secreted by senescent cells [6, 7]. Senomorphics are commonly compounds from natural extraction or chemical synthesis, but most of these compounds

# These authors contributed equally to this work.
* Corresponding author: Yanlan Liu
Mailing address: Molecular Science and Biomedicine Laboratory (MBL), State Key Laboratory of Chemo/Biosensing and Chemometrics, College of Chemistry and Chemical Engineering, Aptamer Engineering Center of Hunan Province, Hunan University, Changsha, Hunan 410082, China.
Email: ylliu@hnu.edu.cn
Received: 29 April 2023 / Revised: 02 June 2023
Accepted: 13 June 2023 / Published: 28 June 2023

lack selectivity for senescent cells and induce adverse effects on normal cells, given the fact that some SASP factors play important roles in many biological processes [7, 8]. Engineering of senotherapeutic prodrugs represents an important alternative strategy to overcome this challenge due to the control of drug activity [9-12]. Previously, researchers have reported a senescence-associated β-galactosidase (SA-β-gal)-activated H_2S donor as an effective senomorphic prodrug [13]. It can be cleaved by the accumulated SA-β-gal in senescent cells, triggering the release of H_2S to alleviate the levels of SASP and reactive oxygen species in senescent cells. Despite the controlled senomorphic activity, SA-β-gal-activated senomorphics still suffer from non-specific activation in some non-senescent cells due to the limitation of using SA-β-gal to distinguish cellular senescence from other cell states with endogenous expression of β-gal [14]. Therefore, strategic innovations are highly needed to further improve the senomorphic selectivity in the regulation of cellular senescence.

To achieve this goal, we design and report a senescent cell-targeted and activatable senomorphic by combining membrane biomarker-mediated active cell recognition with intracellular biomarker-promoted prodrug activation mechanisms. Specifically, an aptamer targeting L1CAM, a transmembrane protein that plays important roles in various cellular processes and is overexpressed in various senescent cells, was selected as the targeting ligand, and SA-β-gal-activated H_2S donor was used as the prodrug moiety to construct a senescence-targeted activatable senomorphic (Apt-H_2SD). Benefiting from the aptamer moiety, Apt-H_2SD shows active targeting and enhanced cellular uptake in senescent cells over proliferating cells. Under the receptor-mediated endocytosis, Apt-H_2SD could be activated in situ by the accumulated SA-β-gal in the lysosomes of senescent cells, triggering the release of H_2S to regulate the SASP signature. Our results suggest that Apt-H_2SD has the potential to be a useful molecular tool for precise intervention in cellular senescence and the related disorders.

Materials and methods

Synthesis of compounds

Compounds 2, and 3 were synthesized according to previously published procedures [9]. To synthesize compound 4, NaH (45 mg, 1.12 mmol) was added to a solution containing compound 3 (200 mg, 0.37 mmol) and p-tolylisothiocyanate (67 mg, 0.45 mmol) in anhydrous tetrahydrofuran (THF) (20 mL) at 0 °C. The mixture was stirred at 0 °C for 30 min and at room temperature for another 4 h. The reaction was quenched with H_2O and extracted with ethyl acetate. The solvent was removed by a rotary evaporator, and the residue was purified by column chromatography to give compound 4 in 48% yield.

For compound 5 (H_2SD), compound 4 (123 mg, 0.18 mmol) was dissolved in a mixture of methanol and dichloromethane (5:3, v/v). Sodium methoxide (65 mg, 1.2 mmol) was then added at 0 °C. The mixture was stirred at 0 °C for 30 min, and the solution was neutralized with Amberlite IRC 50 for 10 min. After removing the solvent with a rotary evaporator, the residue was purified by column chromatography to give compound 5 in 78% yield.

For compound 6 (Apt-H_2SD), azide-modified anti-L1CAM aptamer (50 nmol) was dissolved in 50 μL of ddH_2O and mixed with 50 μL of the TEAA buffer (2 M). 150 mL of dimethylformamide (DMF) containing 500 nmol of compound 5 was added to the above mixture. Then 25 μL of Cu-TBTA complex (10 mM in 55% v/v dimethyl sulfoxide) and 25 μL of ascorbic acid (5 mM) were mixed and added. After stirring for 4 h at 37 °C, the mixture was purified by high performance liquid chromatography (HPLC) to obtain Apt-H_2SD. The HPLC procedures and the DNA sequences used in this study are summarized in Table S1 and Table S2, respectively.

H_2S release experiments

The release of H_2S from H_2SD was determined by a methylene blue (MB) colorimetric assay according to the previous method [13]. Briefly, a 5 mM stock solution of H_2SD was added to PBS containing β-gal (0.5 U/mL) and carbonic anhydrase (CA, 25 μg/mL), followed by incubation at 37 °C with shaking. The MB colorimetric assay was performed, and the absorbance at 670 nm was determined to calculate the release of H_2S. A blank solution without the addition of β-gal was also tested as a reference.

Cell culture

BJ cells were purchased from the American Type Culture Collection (ATCC), and cultured in Dulbecco's modified Eagle's medium (DMEM) with the addition of 10% fetal bovine serum (FBS) and 1% penicillin-streptomycin (PS) in an incubator with a humidified atmosphere of 5% CO_2 at 37 °C.

Senescence induction and characterizations

The hydrogen peroxide (H_2O_2)-induced senescent cell model was established based on previous reports [9, 14, 15]. Briefly, BJ cells were seeded at 6×10^5 cells per well and cultured for 24 h to allow adherence. The cells were then cultured with DMEM containing H_2O_2 (600 μM) for 6 days, after which the medium was replaced with fresh DMEM for subsequent experiments.

To demonstrate the successful induction of senescence, the activity of SA-β-gal in these stimulated cells was first tested using the Senescence β-galactosidase Staining Kit. Briefly, 1×10^5 proliferating or H_2O_2-induced senescent BJ cells were plated in the 6-well plate for 24 h to allow adherence. The cells were then washed and fixed, followed by SA-β-gal staining according to the manufacture's procedures. Finally, the cells were imaged using an inverted microscope (Olympus).

Meanwhile, the cell proliferation ability was examined with 5-ethynyl-2′-deoxyuridine (EdU) assay. Briefly, 1×10^5 BJ cells per well treated with or without H_2O_2 were plated in the 6-well plates. After adherence, the cell proliferation ability was examined according to the manufac-

turer's protocols described and imaged using an inverted microscope.

Cytotoxicity experiments

Cell viability was determined using the Cell Counting Kit-8 (CCK-8) assay. Briefly, 4000 cells per well of proliferating/senescent BJ cells were plated in 96-well plates and cultured for 24h, the cells were incubated with freshly prepared DMEM containing different concentrations of Apt-H_2SD (0, 0.125, 0.25, 0.5, 1, and 2 μM) for 24 h, and then cell viability was assessed using the CCK-8 detection assay.

Cell binding analysis

The ability of Apt-H_2SD to target senescent cells was evaluated by flow cytometry and confocal fluorescence imaging. For flow cytometry, proliferating/senescent BJ cells were digested with 0.2% EDTA and washed twice with PBS. Apt-H_2SD and Con-H_2SD labeled with Cy5 (250 nM) were each incubated with 1.5×10^5 cells in a serum-free DMEM at 4 °C for 45 min. Cells were then centrifuged and washed for flow cytometry (BD FACS Verse).
For confocal fluorescence imaging, proliferating/senescent BJ cells were plated in the confocal dish at 1.0×10^5 cells per well. After 24 h of culture, the cells were washed twice with PBS and cultured with 200 μL of serum-free DMEM containing 250 nM Cy5-Apt-H_2SD/Con-H_2SD for 45 min at 4 °C. The cells were then washed and stained with Hoechst. Cellular fluorescence was examined by laser scanning confocal microscopy (FV1000 confocal microscope, Olympus).

SASP inhibition analysis

The expression of SASP in senescent BJ cells treated with or without Apt-H_2SD was examined at the mRNA level by reverse transcription quantitative real-time PCR (RT-qPCR). After treatment with Apt-H_2SD, all the experimental procedures were referred to the previous report [9,13]. Primers used in this experiment are summarized in Table S3.

Statistical Analysis

All data were presented as mean ± standard deviation (SD). The difference between two groups was compared by using the Student's t-test. The difference among multiple groups was compared by using the one-way analysis of variance (ANOVA) followed by the LSD (Tukey's) post hoc test. Differences were considered statistically significant if $P < 0.05$.

Results

The synthesis of Apt-H_2SD is shown in Figure 1. The glycosylated intermediate (compound 3) was first synthesized following previous work [9], providing an ideal platform for conjugation of the H_2S-donating moiety at the benzylic position and the targeting ligand at the terminal alkyne. Subsequent conjugation with p-tolylisothiocyanate and deprotection of the hydroxy groups yielded the cleavable compound 5 (H_2SD). In the presence of SA-β-gal, H_2SD could release carbonyl sulfide (COS), which would be rapidly converted to H_2S by the ubiquitous enzyme carbonic anhydrase (CA) inside the senescent cells to execute the SASP regulation. Finally, anti-L1CAM aptamer

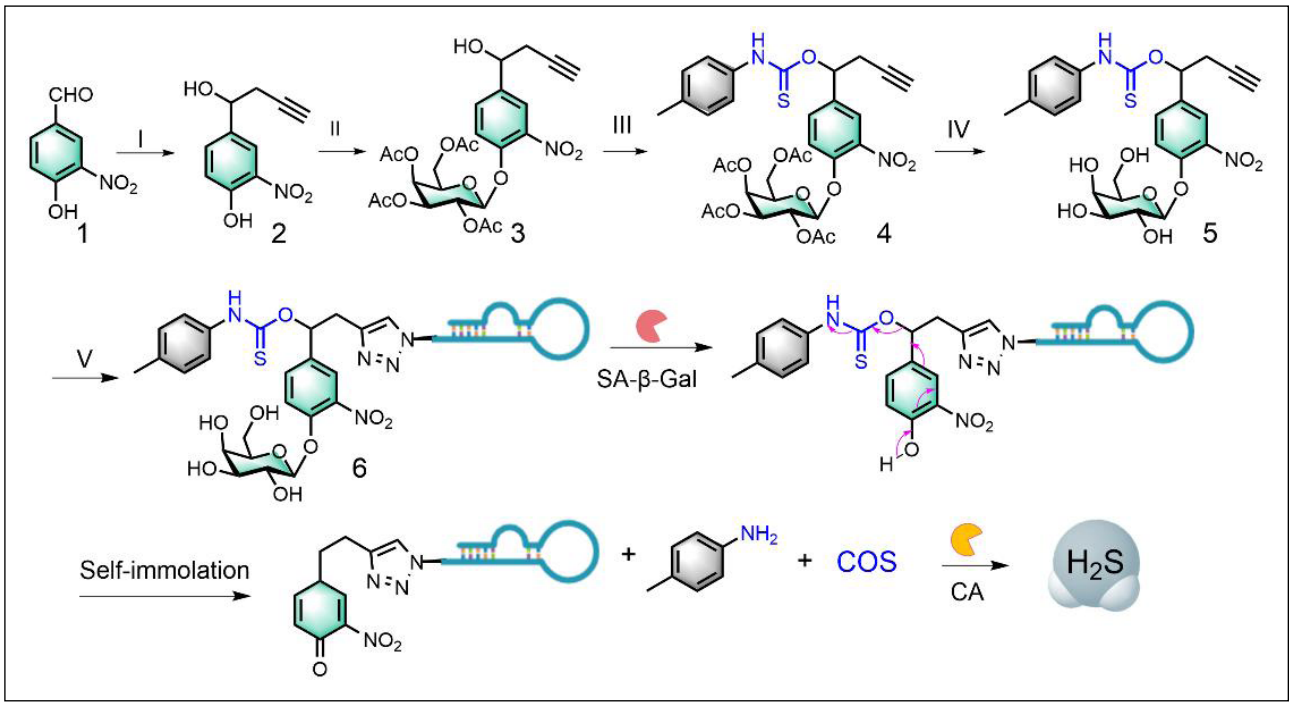

Figure 1. Synthetic route to Apt-H_2SD and its H_2S release mechanism. Reagents and conditions: (**I**) propargyl bromide, Al, $HgCl_2$, THF; (**II**) Ag_2CO_3, 1,1,4,7,10,10-hexamethyltriethylenetetramine, 2,3,4,6-tetra-O-acetyl-α-d-galactopyranosyl bromide, CH_3CN, rt; (**III**) P-tolylisothiocyanate, NaH, THF; (**IV**) CH_3OH, CH_3ONa. (**V**) $CuSO_4$, sodium ascorbate, N_3-labeled anti-L1CAM aptamer, DMF/H_2O. Detailed synthesis can be found in the method section.

was conjugated at the tail via click chemistry to yield the senescence-targeted activatable molecular senomorphic (Apt-H_2SD). All the intermediates were characterized by NMR spectra, and Apt-H_2SD was characterized by MS (Figure S1-S9).

With H_2SD in hand, we proceeded to investigate its enzyme-responsive and H_2S-releasing capabilities. In the presence of β-gal and carbonic anhydrase via methylene blue assay. As shown in Figure 2, H_2SD exhibited rapid release of H_2S upon incubation in the PBS buffer containing β-gal and CA, and the reaction was almost complete within 2 h, with a release efficiency of about 50%. In sharp contrast, no H_2S production was detected in the absence of β-gal within the same time period, suggesting that the presence of CA alone did not induce the cleavage of thiocarbamates. Collectively, these results confirmed the β-gal-activated property of H_2SD.

Having confirmed the controllable activity, we next asked whether Apt-H_2SD could achieve targeted recognition of senescent cells. As a proof-of-concept, oxidative stress-induced cellular senescence was established using BJ cells as the model and H_2O_2 as the stress. SA-β-gal staining results showed that after stimulation with H_2O_2, BJ cells exhibited obvious enlargement in the cell volume, coupled with blue staining (Figure 3A), indicating the accumulation of SA-β-gal. 5-Ethynyl-2′-deoxyuridine (EdU)-based cell proliferation assay further confirmed that these stressed BJ cells lost the proliferative ability, as evidenced by the negative EdU staining (Figure 3B). On the other hand, we have also examined the levels of three senescence-associated markers, including p16, p21, and IL-1β, in these stimulated cells. The results showed a significant elevation in the expression of these markers at the mRNA level (Figure S10). Furthermore, the upregulation of L1CAM in senescent BJ cells was verified by Western blot analysis (Figure 3C).

Next, the cell recognition ability of Apt-H_2SD towards senescent cells was evaluated by flow cytometry and confocal fluorescence imaging. As shown in Figure 3D, H_2O_2-induced senescent BJ cells exhibited a significant shift in fluorescence intensity after incubation with Cy5-labeled Apt-H_2SD compared to proliferating BJ cells. Moreover, such fluorescence shift in senescent BJ cells treated with Cy5-labeled Apt-H_2SD was much greater than that in senescent cells treated with Cy5-labeled non-targeting Con-H_2SD, suggesting that Apt-H_2SD could selectively recognize senescent cells over proliferating cells. Consistent with the flow cytometry results, confocal imaging further confirmed the senescent cell targeting ability of Apt-H_2SD. Among the different treatment groups, only senescent cells treated with Cy5-labeled Apt-H_2SD showed bright red fluorescence (Figure 3E). To confirm whether Apt-H_2SD accumulated in lysosomes of senescent cells, lysosomal colocalization analysis was performed. Senescent BJ cells were treated with Cy5-labeled Apt-H_2SD and stained with Lysotracker Green, followed by confocal fluorescence imaging. As we expected, a large overlap between the green and red fluorescence channels was observed (Figure 3F), suggesting the lysosomal accumulation of Apt-H_2SD in senescent cells.

Having identified the cell targeting property, we next evaluated the senomorphic activity of Apt-H_2SD in suppressing the secretion of SASP in senescent cells (Figure 4). When BJ cells were stimulated with H_2O_2, the expression of proinflammatory interleukins (IL-6 and IL-1β) and matrix metalloproteinases 3 (MMP3) were upregulated compared to untreated cells. Interestingly, Apt-H_2SD could attenuate the expression of these SASP factors. On the other hand, Apt-H_2SD showed good biocompatibility without causing adverse effects on proliferation and growth in non-senescent cells at the concentrations tested (Figure S11).

Discussion

Cellular senescence is a complex cellular stress response triggered by endogenous and/or exogenous stimuli [15].

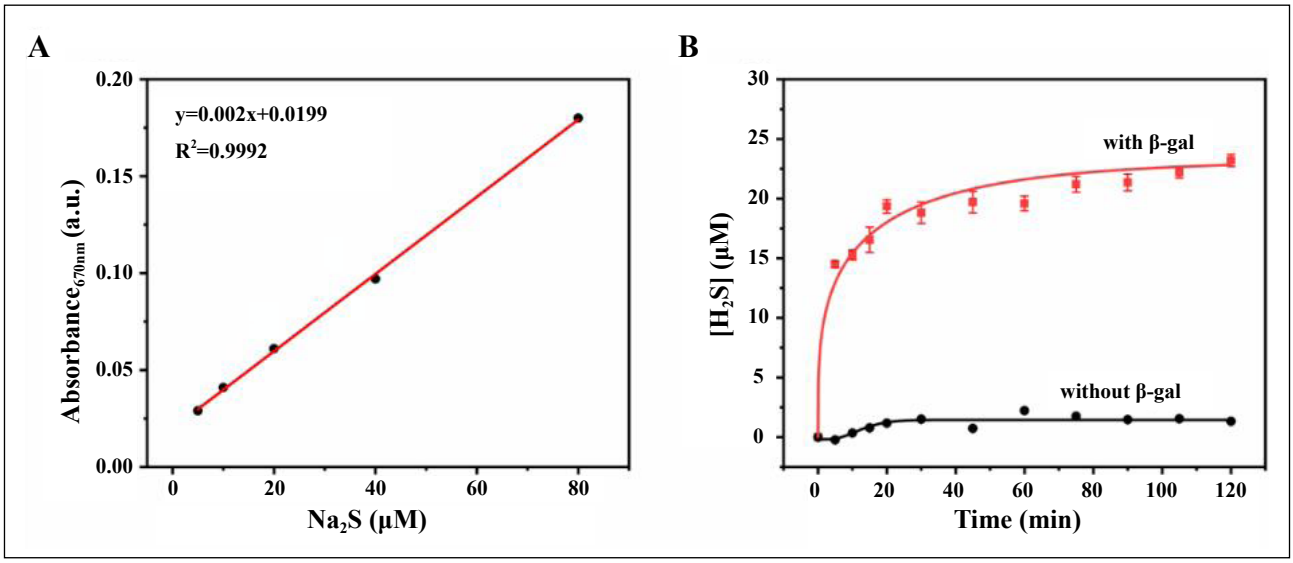

Figure 2. (**A**) The standard curve for the measurement of H_2S using the methylene blue (MB) method and Na_2S as the standard. (**B**) Time-dependent H_2S release from H_2SD in the presence vs. absence of β-gal, as measured by the MB assay.

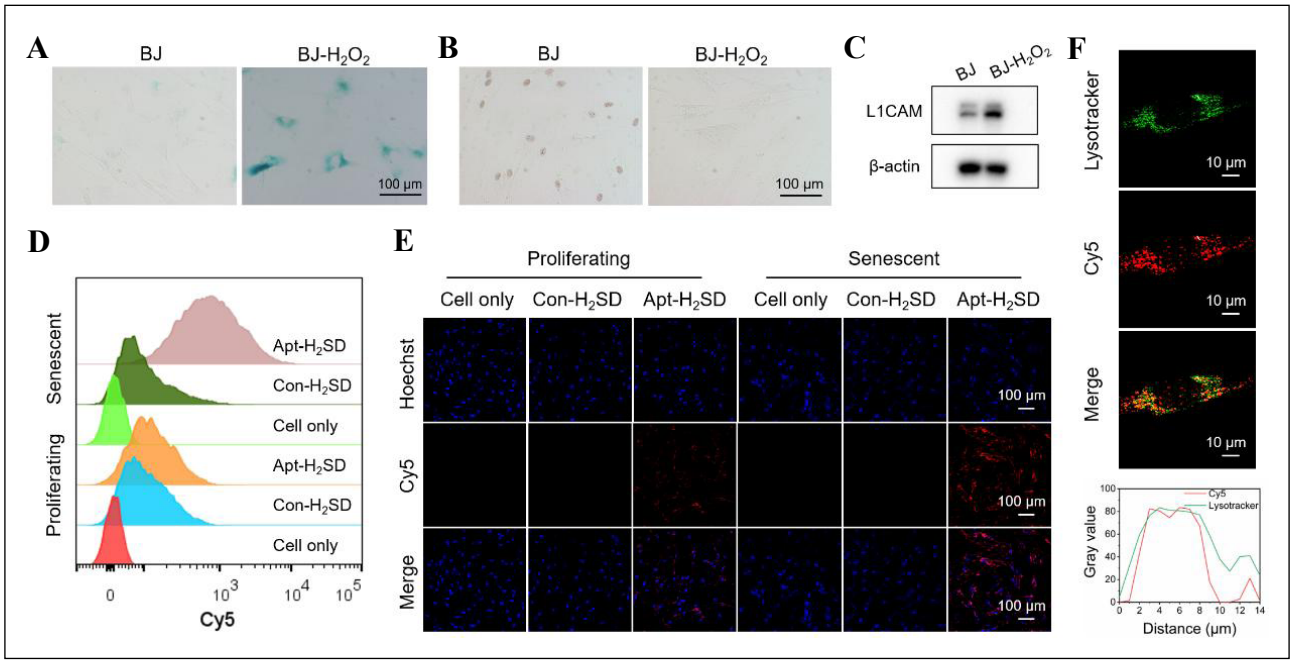

Figure 3. (**A**) SA-β-gal staining and (**B**) EdU staining images of proliferating BJ cells and H_2O_2-induced senescent BJ cells, respectively. (**C**) Western blot analysis of L1CAM expression in proliferating BJ cells and senescent BJ cells. (**D**) Flow cytometry analysis and (**E**) confocal imaging of proliferating BJ cells and senescent BJ cells after incubation with Cy5-labeled Apt-H_2SD and Con-H_2SD, respectively. (**F**) Lysosomal colocalization analysis of Cy5-labeled Apt-H_2SD in senescent BJ cells.

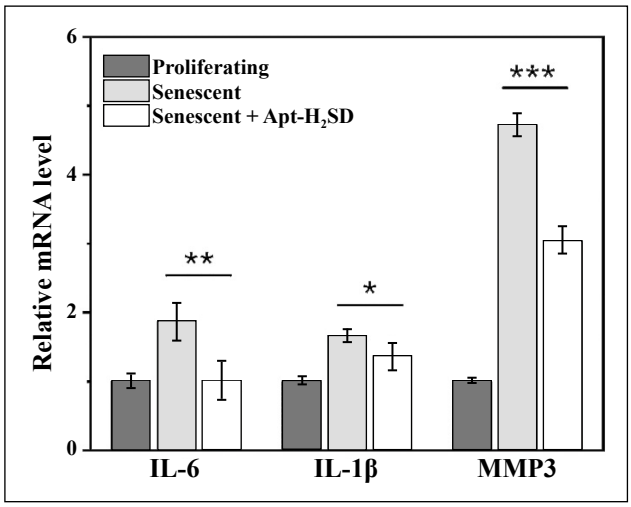

Figure 4. Expression of IL-6, IL-1β, and MMP3 at the mRNA level in proliferating BJ cells and H_2O_2-induced senescent BJ cells after exposure to Apt-H_2SD. Data are presented as mean ± SD (n = 3). $^*P < 0.05$, $^{**}P < 0.01$, and $^{***}P < 0.001$.

Despite the loss of the proliferative capacity, senescent cells remain metabolically active and retain the potential to secrete various types of SASP (*e.g.*, pro-inflammatory cytokines, growth factors, chemokines, and matrix-degrading enzymes) [16]. These signaling molecules can reprogram the tissue microenvironment and induce inflammation, which in turn promotes second senescence in surrounding cells, cumulatively driving aging and age-related diseases such as cancer, cardiovascular disease, and neurodegenerative disorders [17, 18]. Thus, SASP has recently emerged as a therapeutic target for age-related diseases, and studies have shown that selective regulation of SASP with senomorphics is an important strategy to delay the aging process and age-related diseases or to improve disease treatment [19]. Traditionally, senomorphics are discovered by high-throughput screening of large libraries composed of small chemicals and natural products. The activity of these agents has been uncontrolled, which can interfere with the signaling pathways in normal cells, resulting in unwanted side effects [8, 20]. Although SA-β-gal-activated senomorphics have been developed to improve the selectivity of senescent cells, precise intervention in cellular senescence is still a major challenge because β-gal is expressed not only in senescent cells but also in certain normal cells and proliferating cancer cells. Therefore, there is an urgent need to develop targeted approaches with enhanced specificity and efficacy for SASP regulation during senescence.

Therefore, this work aimed to improve the applicability of senomorphic-based anti-senescence methods, and reported a novel class of senomorphics, designated Apt-H_2SD, with active cell recognition and activatable senomorphic activity, by taking advantage of aptamer-prodrug conjugation strategy. The senomorphic activity of Apt-H_2SD can be switched by SA-β-gal-catalyzed cleavage of the molecular structure, resulting in release of the H_2S donor and subsequent conversion of H_2S by carbonic anhydrase (Figure 2), a ubiquitous enzyme in various mammalian cells. As a proof of concept, BJ cells, a normal human fibroblast cell line, were selected as a model cell to establish the model of cellular senescence, given the fact that fibroblast senescence contributes to the organic aging and the pathology of many important diseases, such as, pulmonary fibrosis, cancer, neurodegeneration, and cardiac diseases [21-28]. The feasibility of Apt-H_2SD to regulate SASP was investigated in oxidative stress-induced senescent BJ cells. Cell

binding studies showed that Apt-H_2SD could selectively target and accumulate in senescent BJ cells over proliferating cells through the aptamer-mediated cell recognition (Figure 3). More impressively, treatment with Apt-H_2SD could downregulate the expression of three types of important SASP factors in senescent cells (Figure 4), suggesting its potential for cell-specific SASP regulation. The graphical summary is shown in Figure 5. Nevertheless, more in-depth studies, such as its influence on the secretion of other types of SASP, the expression of SASP at the genetic level, and the duration of action, are still needed to better evaluate the performance of Apt-H_2SD and to elucidate the exact mechanisms underlying the SASP regulation.

Conclusion

Although the research we present here is relatively preliminary, its scientific applications are potentially broad, as cellular senescence not only contributes to aging, but is highly implicated in the initiation and the initiation and progress of many important diseases. Such an aptamer-prodrug conjugation strategy may also pave the way for the design and construction of various senomorphics by altering the drug moiety, which is expected to have a profound impact on the treatment and prevention of age-related diseases.

Declarations

Authors' contributions: Yuqi Xie, Jili Li, and Yanlan Liu conceptualized and planned the work leading to the manuscript; Yuqi Xie, Jili Li, Pingyu Wu, Linlin Wang, Donghui Hong, and Jian Wang collected and analyzed the data; Yuqi Xie, Jili Li, and Yanlan Liu drafted the manuscript. The final version of the manuscript was reviewed and approved by all the authors.

Availability of data and materials: The data supporting the study results are available from the corresponding author upon reasonable request.

Financial support and sponsorship: This study was supported by the National Key Research and Development Program of China (Grant No. 2020YFA0210802), the National Natural Science Foundation of China (Grant Nos. NSFC22274044 and 21877031), and the Science and Technology Innovation Program of Hunan Province (Grant No. 2018RS3043).

Conflicts of interest: The authors declare no competing financial interests.

Ethical approval and consent to participate: Not applicable.

References

1. Acklin S, Zhang M, Du W, Zhao X, Plotkin M, Chang J, *et al*. Depletion of senescent-like neuronal cells alleviates cisplatin-induced peripheral neuropathy in mice. *Sci Rep*, 2020, 10(1): 14170. [Crossref]
2. Childs BG, Durik M, Baker DJ, & van Deursen JM. Cellular senescence in aging and age-related disease: from mechanisms to therapy. *Nat Med*, 2015, 21(12): 1424-

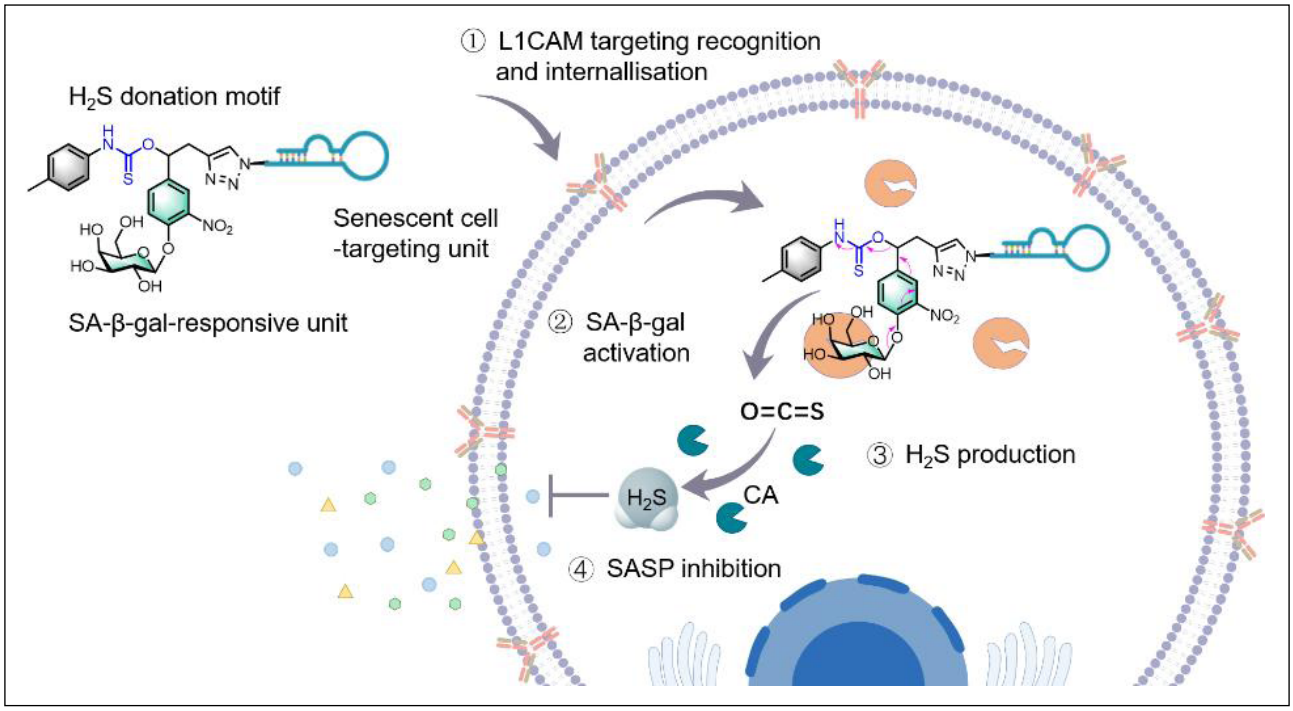

Figure 5. A senescent cell-targeted and activatable H_2S donor (Apt-H_2SD) is developed as an innovative senomorphic mediated by aptamer-mediated active cell recognition and senescence-associated enzyme-triggered activation mechanisms. Such a design allows the selective accumulation and activation of Apt-H_2SD in senescent cells over proliferating cells, contributing to the release of H_2S to attenuate the secretion of the senescence-associated secretory phenotype (SASP).

1435. [Crossref]
3. Chen H, Ruiz PD, McKimpson WM, Novikov L, Kitsis RN, & Gamble MJ. MacroH2A1 and ATM play opposing roles in paracrine senescence and the senescence-associated secretory phenotype. *Mol Cell*, 2015, 59(5): 719-731. [Crossref]
4. Martel J, Ojcius DM, Wu CY, Peng HH, Voisin L, Perfettini JL, *et al*. Emerging use of senolytics and senomorphics against aging and chronic diseases. *Med Res Rev*, 2020, 40(6): 2114-2131. [Crossref]
5. Tchkonia T, Zhu Y, van Deursen J, Campisi J, & Kirkland JL. Cellular senescence and the senescent secretory phenotype: therapeutic opportunities. *J Clin Invest*, 2013, 123(3): 966-972. [Crossref]
6. Lozono-Torres B, Estepa-Fernandez A, Rovira M, Orzaez M, Serrano M, Martinez-Manez R, *et al*. The chemistry of senescence. *Nat Rev Chem*, 2019, 3(7): 426-441. [Crossref]
7. Zhang L, Pitcher LE, Prahalad V, Niedernhofer LJ, & Robbins PD. Targeting cellular senescence with senotherapeutics: senolytics and senomorphics. *FEBS J*, 2023, 290(5): 1362-1383. [Crossref]
8. Lagoumtzi SM, & Chondrogianni N. Senolytics and senomorphics: natural and synthetic therapeutics in the treatment of aging and chronic diseases. *Free Radical Bio Med*, 2021, 171: 169-190. [Crossref]
9. Xia Y, Li J, Wang L, Luo X, Xie Y, & Liu Y. Spatially confined intervention of cellular senescence by a lysosomal metabolism targeting molecular prodrug for broad-spectrum senotherapy. *Angew Chem Int Ed Engl*, 2022, 61(12): e202115764. [Crossref]
10. Gonzalez-Gualda E, Paez-Ribes M, Lozano-Torres B, Macias D, Wilson III, Gonzalez-Lopez C, *et al*. Galacto-conjugation of Navitoclax as an efficient strategy to increase senolytic specificity and reduce platelet toxicity. *Aging Cell*, 2020, 19(4): e13142. [Crossref]
11. Guerrero A, Guiho R, Herranz N, Uren A, Withers DJ, Martinez-Barbera JP, *et al*. Galactose-modified duocarmycin prodrugs as senolytics. *Aging Cell*, 2020, 19(4): e13133. [Crossref]
12. Cai Y, Zhou H, Zhu Y, Sun Q, Ji Y, Xue A, *et al*. Elimination of senescent cells by beta-galactosidase-targeted prodrug attenuates inflammation and restores physical function in aged mice. *Cell Res*, 2020, 30(7): 574-589. [Crossref]
13. Li J, Xie Y, Wang J, Wang L, Xia Y, Liu Y, *et al*. Activatable and self-monitoring hydrogen sulfide-based molecular senomorphics for visualized regulation of cellular senescence. *CCS Chemistry*, 2023: 1-28. [Crossref]
14. Li JL, Wang LL, Luo XY, Xia YH, Xie YQ, Liu YL, *et al*. Dual-parameter recognition-directed design of the activatable fluorescence probe for precise imaging of cellular senescence. *Anal Chem*, 2023, 95(8): 3996-4004. [Crossref]
15. Hernandez-Segura A, Nehme J, & Demaria M. Hallmarks of cellular senescence. *Trends Cell Biol*, 2018, 28(6): 436-453. [Crossref]
16. Hayakawa T, Iwai M, Aoki S, Takimoto K, Maruyama M, Maruyama W, *et al*. SIRT1 suppresses the senescence-associated secretory phenotype through epigenetic gene regulation. *Plos One*, 2015, 10(1): e0116480. [Crossref]
17. Freund A, Orjalo AV, Desprez PY, & Campisi J. Inflammatory networks during cellular senescence: causes and consequences. *Trends Mol Med*, 2010, 16(5): 238-246. [Crossref]
18. Niedernhofer LJ, & Robbins PD. Senotherapeutics for healthy ageing. *Nat Rev Drug Discov*, 2018, 17(5): 377-380. [Crossref]
19. Guo J, Huang X, Dou L, Yan M, Shen T, Tang W, *et al*. Aging and aging-related diseases: from molecular mechanisms to interventions and treatments. *Signal Transduct Target Ther*, 2022, 7(1): 391-431. [Crossref]
20. Raffaele M, & Vinciguerra M. The costs and benefits of senotherapeutics for human health. *Lancet Glob Health*, 2022, 3(1): E67-E77. [Crossref]
21. Kortlever RM, Higgins PJ, & Bernards R. Plasminogen activator inhibitor-1 is a critical downstream target of p53 in the induction of replicative senescence. *Nat Cell Biol*, 2006, 8(8): 877-884. [Crossref]
22. Li M, Yang X, Lu X, Dai N, Zhang S, Cheng Y, *et al*. APE1 deficiency promotes cellular senescence and premature aging features. *Nucleic Acids Res*, 2018, 46(11): 5664-5677. [Crossref]
23. Eberhardt K, Beleites C, Marthandan S, Matthäus C, Diekmann S, & Popp J. Raman and infrared spectroscopy distinguishing replicative senescent from proliferating primary human fibroblast cells by detecting spectral differences mainly due to biomolecular alterations. *Anal Chem*, 2017, 89(5): 2937-2947. [Crossref]
24. Keys B, Serra V, Saretzki G, & Von Zglinicki T. Telomere shortening in human fibroblasts is not dependent on the size of the telomeric-3'-overhang. *Aging Cell*, 2004, 3(3): 103-109. [Crossref]
25. Meyer K, Hodwin B, Ramanujam D, Engelhardt S, & Sarikas A. Essential role for premature senescence of myofibroblasts in myocardial fibrosis. *J Am Coll Cardiol*, 2016, 67(17): 2018-2028. [Crossref]
26. Bavik C, Coleman I, Dean JP, Knudsen B, Plymate S, & Nelson PS. The gene expression program of prostate fibroblast senescence modulates neoplastic epithelial cell proliferation through paracrine mechanisms. *Cancer Res*, 2006, 66(2): 794-802. [Crossref]
27. Franco AC, Aveleira C, & Cavadas C. Skin senescence: mechanisms and impact on whole-body aging. *Trends Mol Med*, 2022, 28(2): 97-109. [Crossref]
28. Sawaki D, Czibik G, Pini M, Ternacle J, Suffee N, Mercedes R, *et al*. Visceral adipose tissue drives cardiac aging through modulation of fibroblast senescence by osteopontin production. *Circulation*, 2018, 138(8): 809-822. [Crossref]

Cite this article as: Xie Y, Li J, Wu P, Wang L, Hong D, Wang J, *et al*. Targeted regulation of senescence-associated secretory phenotype with an aptamer-conjugated activatable senomorphic. *Aging Pathobiol Ther*, 2023, 5(2): 59-65. doi: 10.31491/APT.2023.06.113

Table S1. DNA sequences used in this study.

Name	Detailed sequence information (5'-3')
N3-Aptamer	N3-AGGATAGGGGGTAGCTCGGTCGTGTTTTTGGG TTGTTTGGTGGGTCTTCTG
N3-Aptamer-Cy5	N3-AGGATAGGGGGTAGCTCGGTCGTGTTTTTGGG TTGTTTGGTGGGTCTTCTG-Cy5
N3-Control DNA-Cy5	N3- (T) 51- Cy5

Table S2. HPLC procedures used in this study.

Tmie/min	Eluent A (0.1 M TEAA)	Eluent B (Acetonitrile)
0	95%	5%
4	95%	5%
4.01	90%	10%
30	35%	65%

Table S3. The primary DNA sequences used in this work.

Gene	Forward (5'-3')	Reverse (5'-3')
P16	GCTGCCCAACGCACCGAATA	ACCACCAGCGTGTCCA
P21	GACAGCAGAGGAAGACCATGTGGAC	GAGTGGTAGAAATCTGTCATGCTG
IL-6	CCAGGAGCCCAGCTATGAAC	CCCAGGGAGAAGGCAACTG
IL-1β	CTGTCCTGCGTGTTGAAAGA	TTGGGTAATTTTTGGGATCTACA
MMP3	AGGGAACTTGAGCGTGAATC	TCACTTGTCTGTTGCACACG
GADPH	GAAGGTGAAGGTCGGAGTC	TTGAGGTCAATGAAGGGG

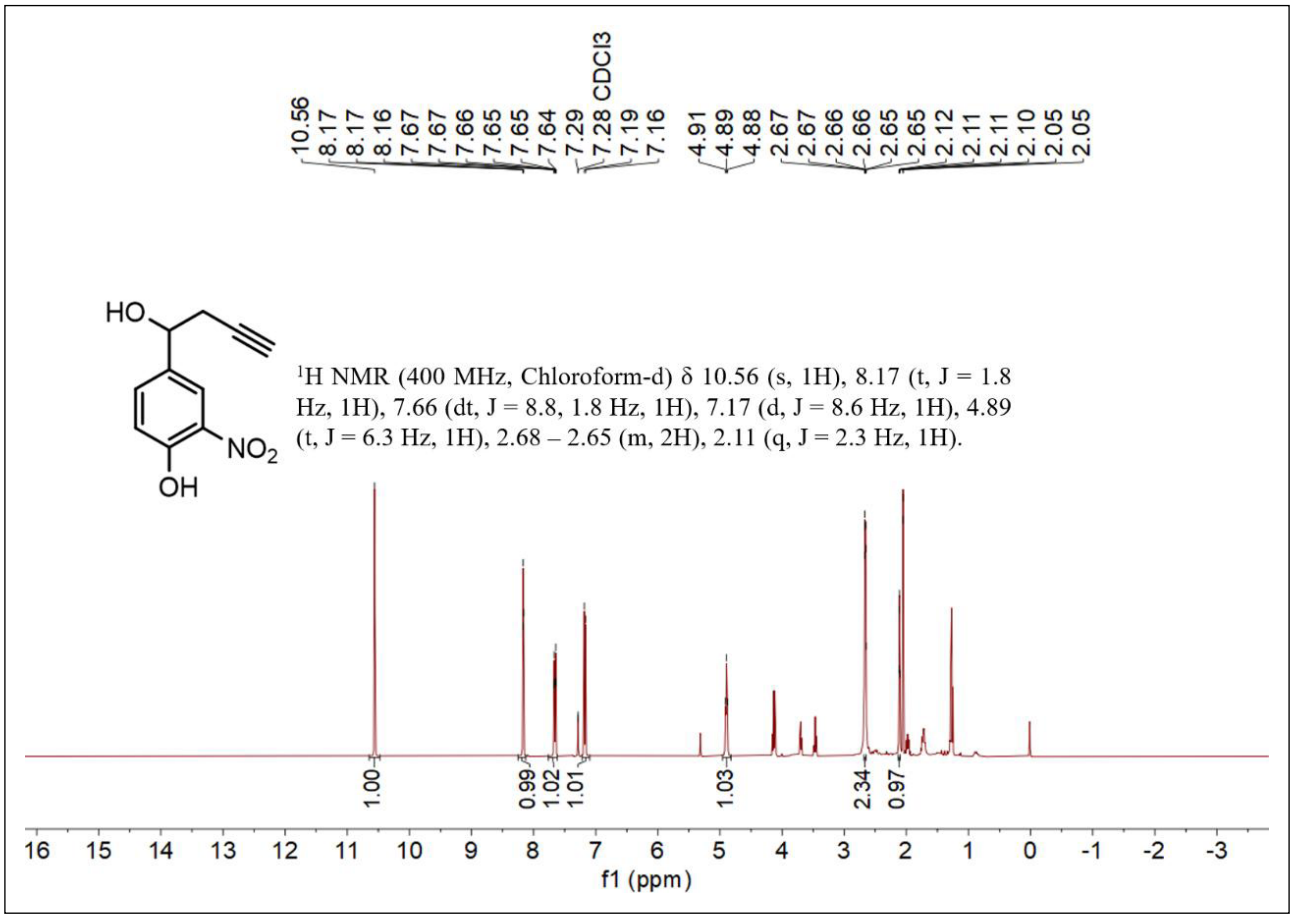

Figure S1. ^{1}H NMR spectrum of compound 2.

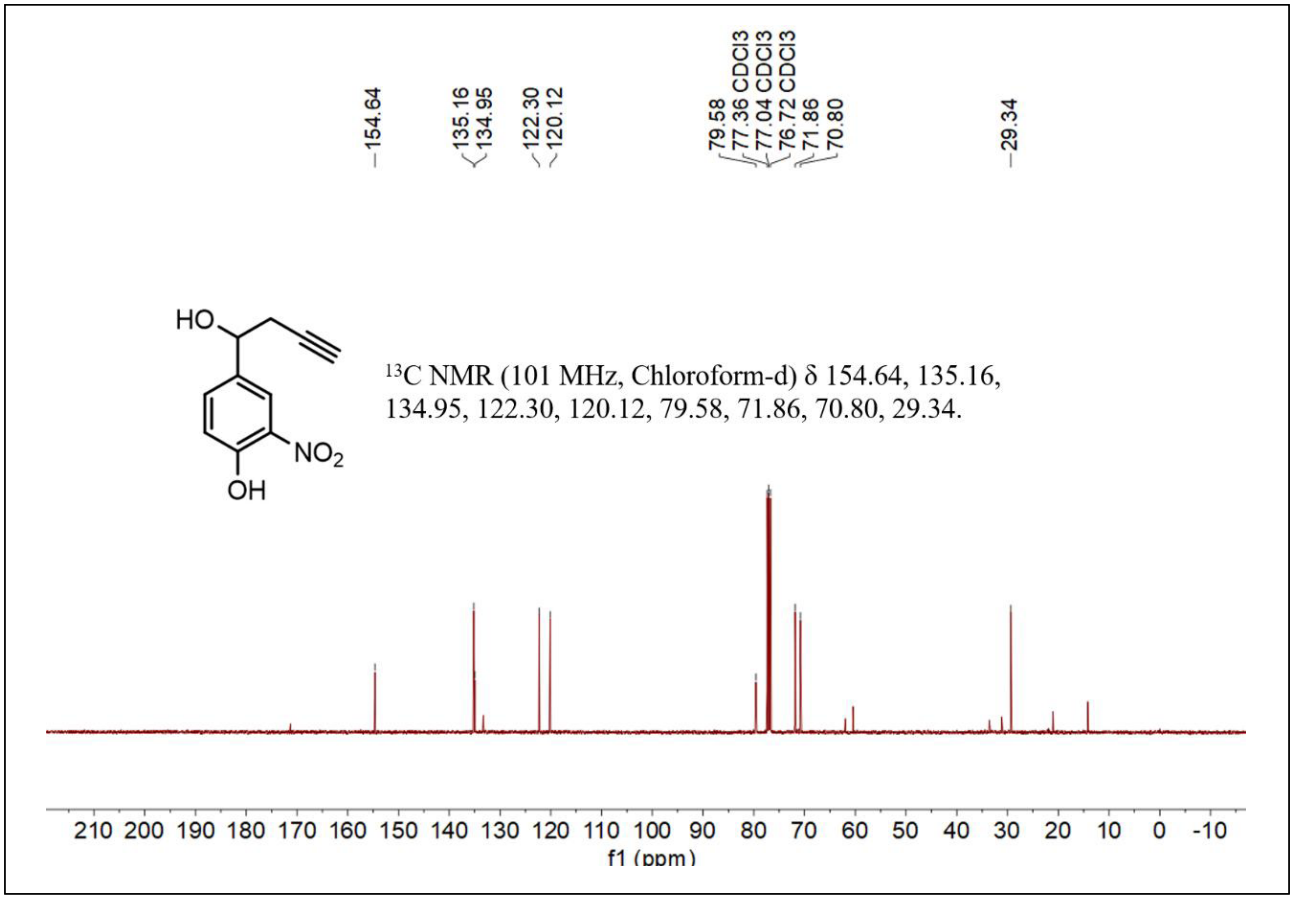

Figure S2. ^{13}C NMR spectrum of compound 2.

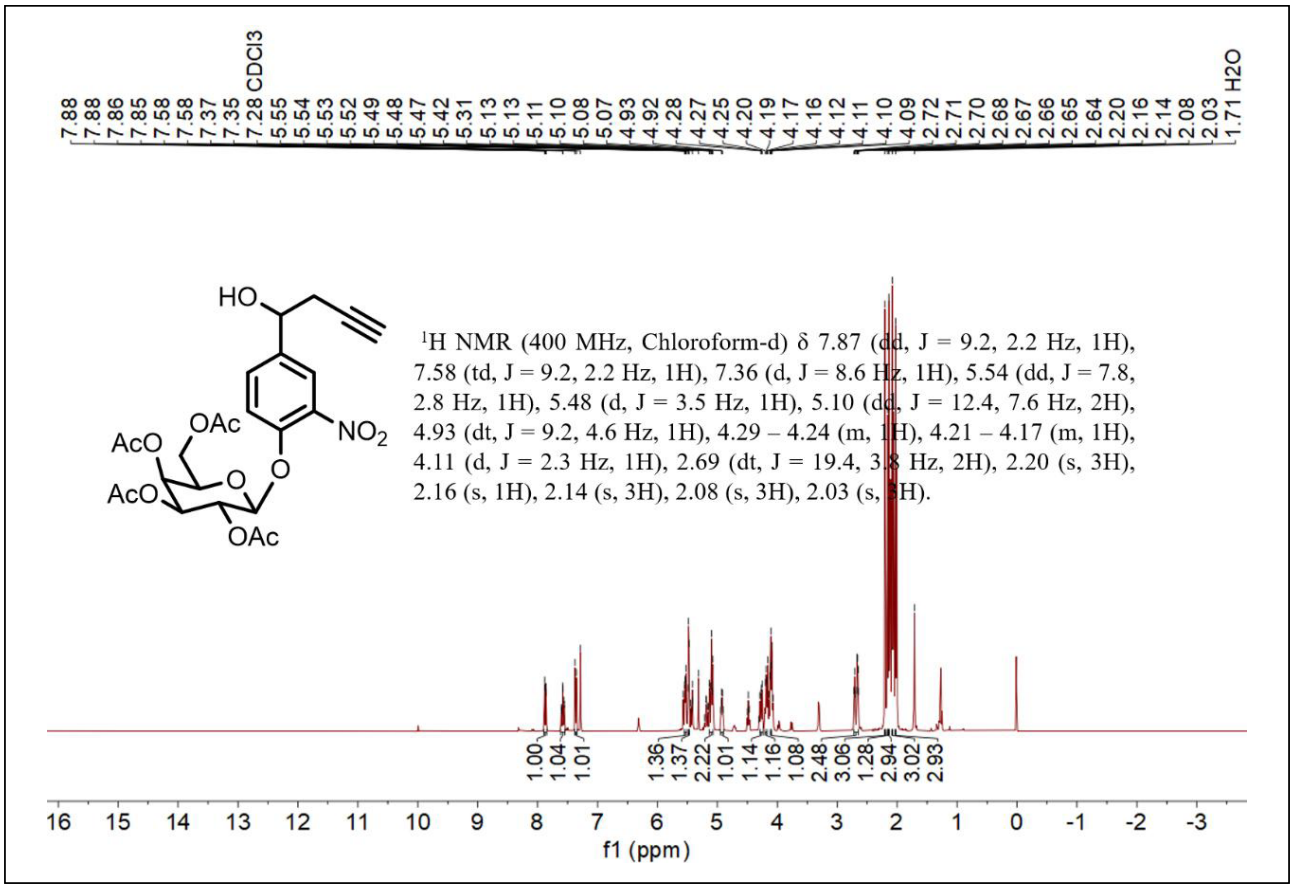

Figure S3. ^{1}H NMR spectrum of compound 3.

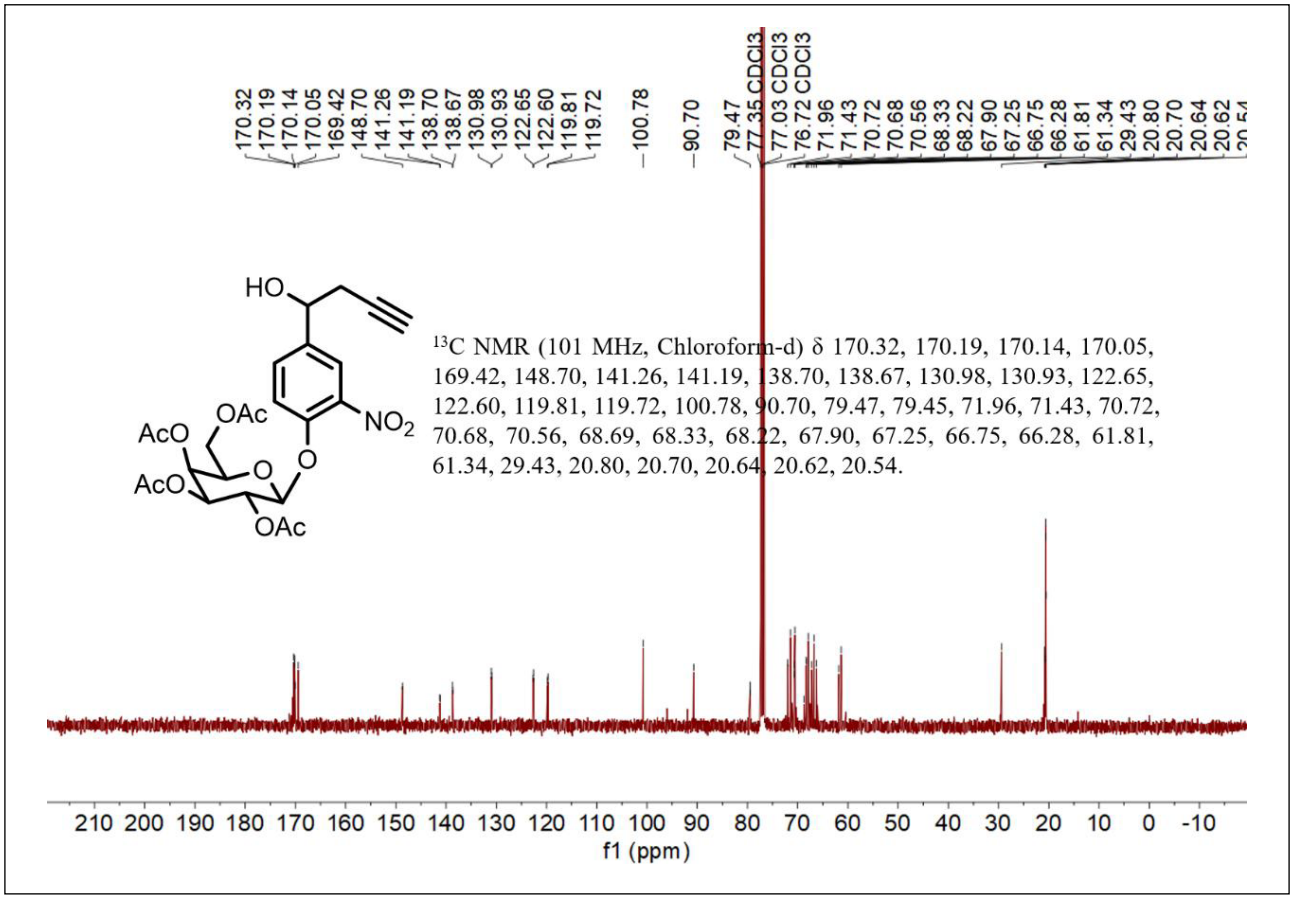

Figure S4. ^{13}C NMR spectrum of compound 3.

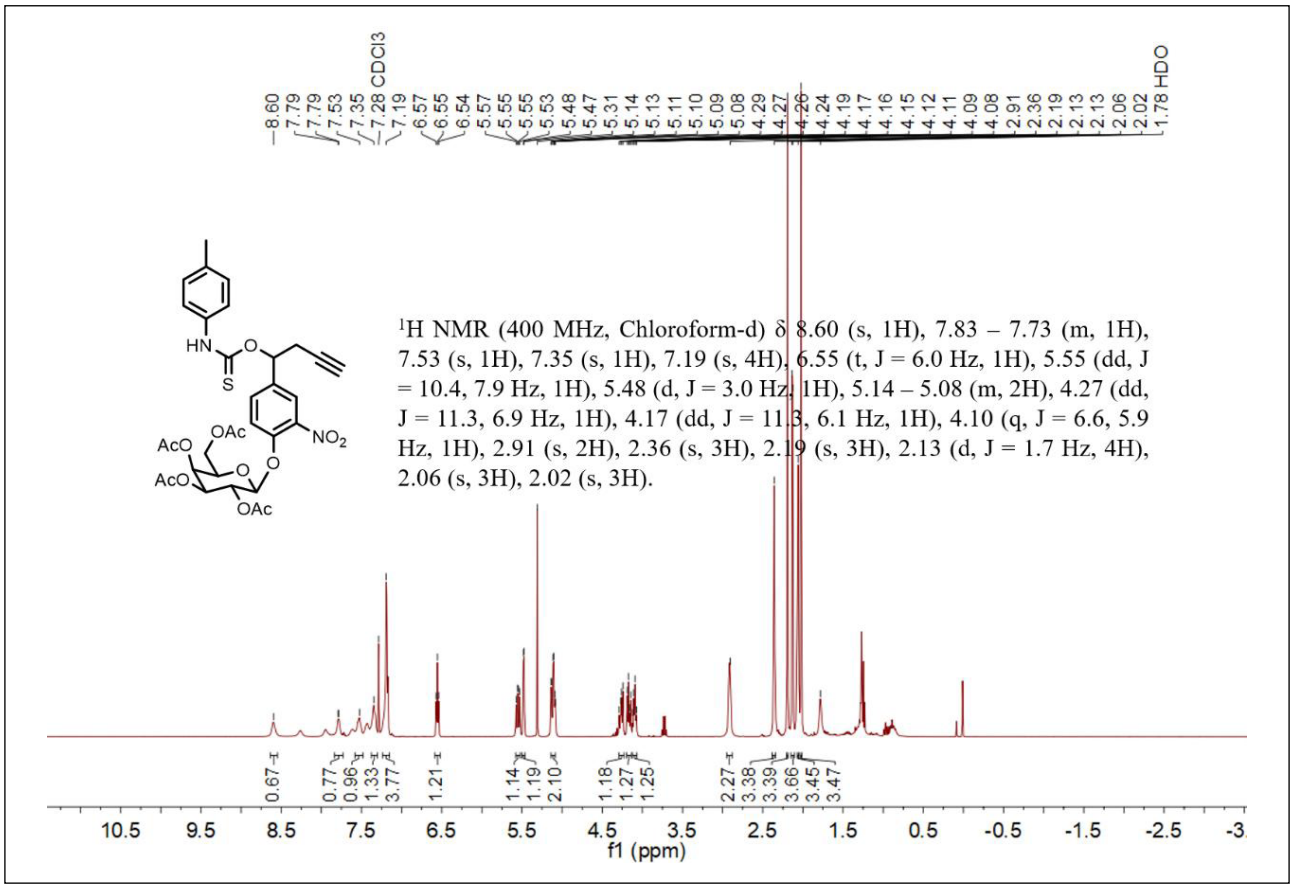

Figure S5. ^{1}H NMR spectrum of compound 4.

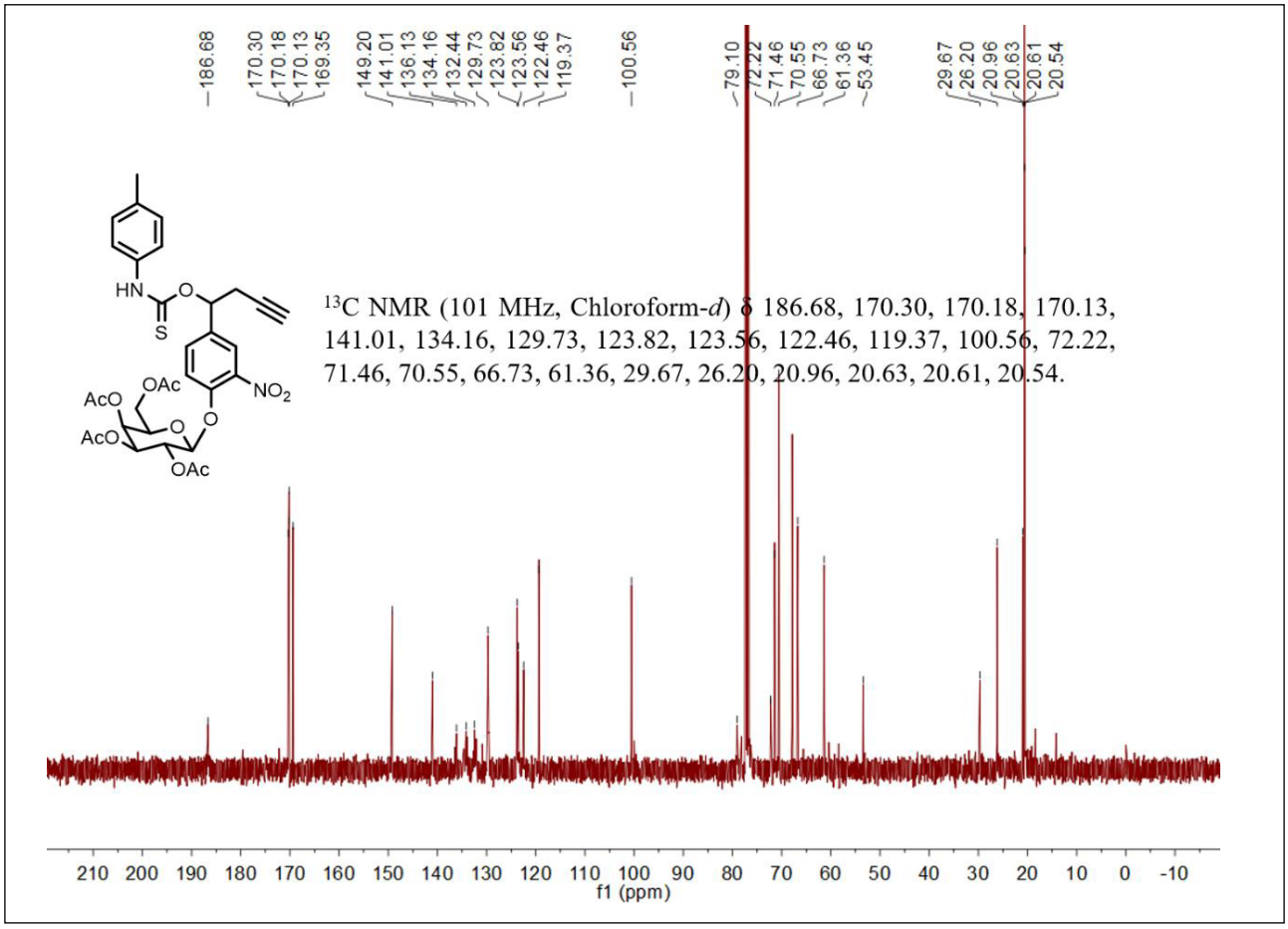

Figure S6. ^{13}C NMR spectrum of compound 4.

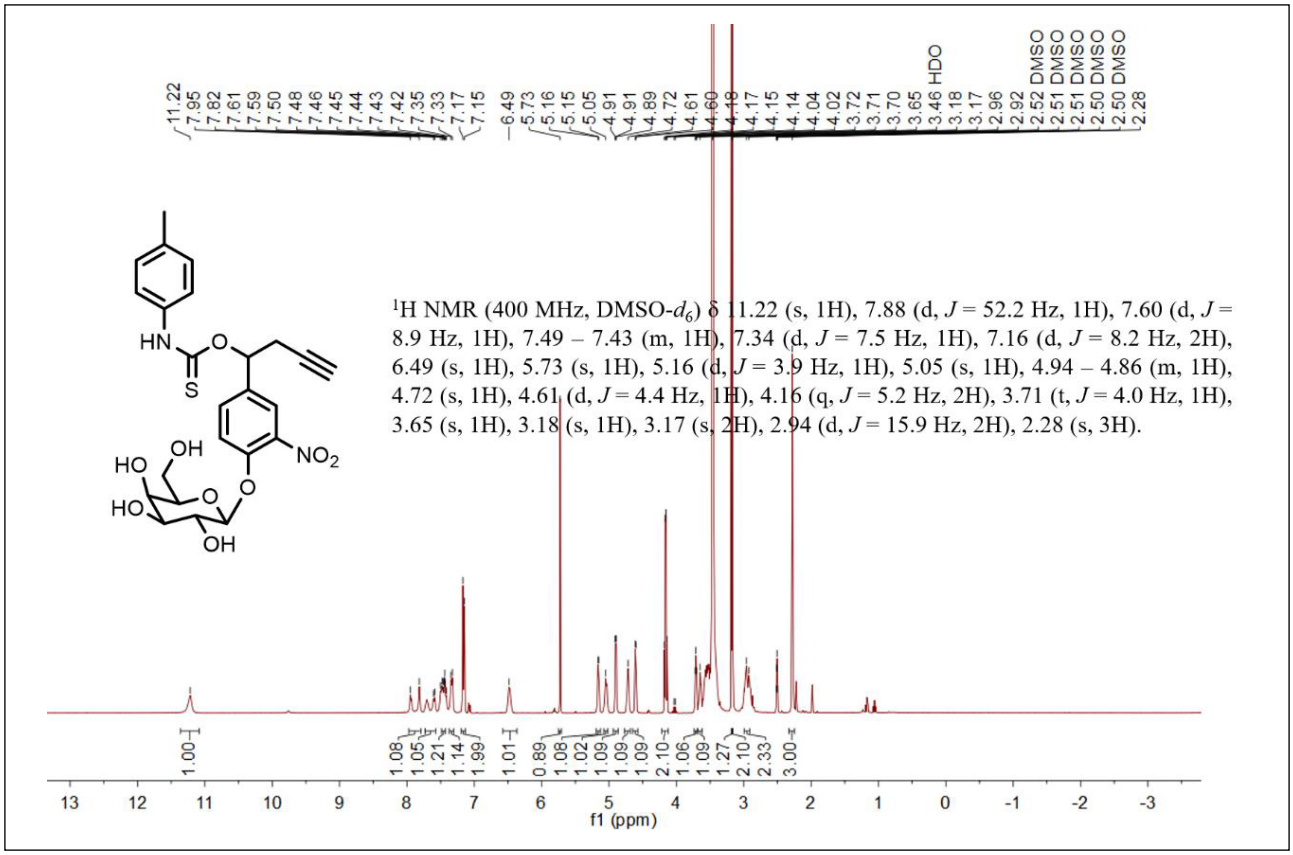

Figure S7. ^{1}H NMR spectrum of compound 5.

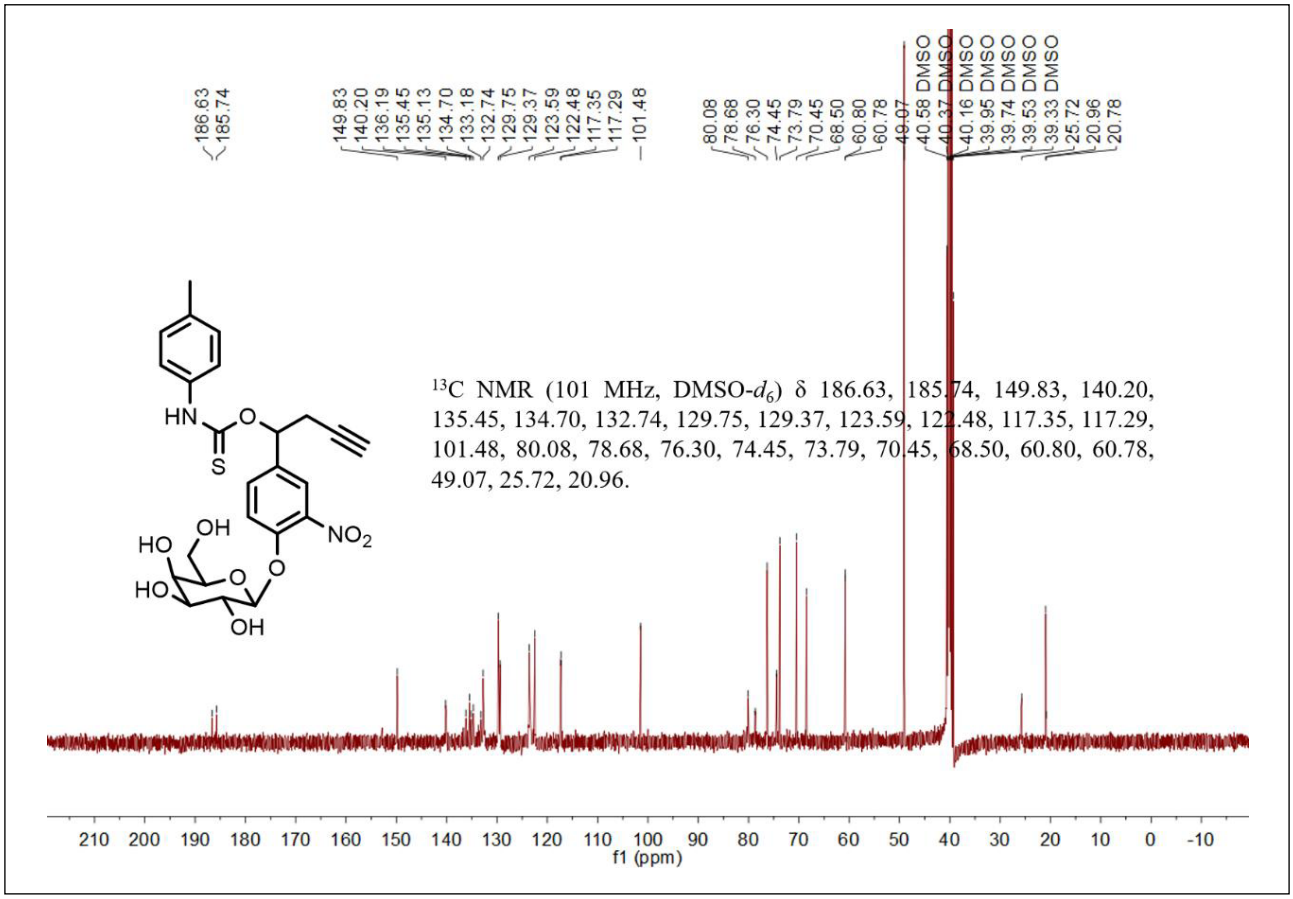

Figure S8. ^{13}C NMR spectrum of compound 5**.**

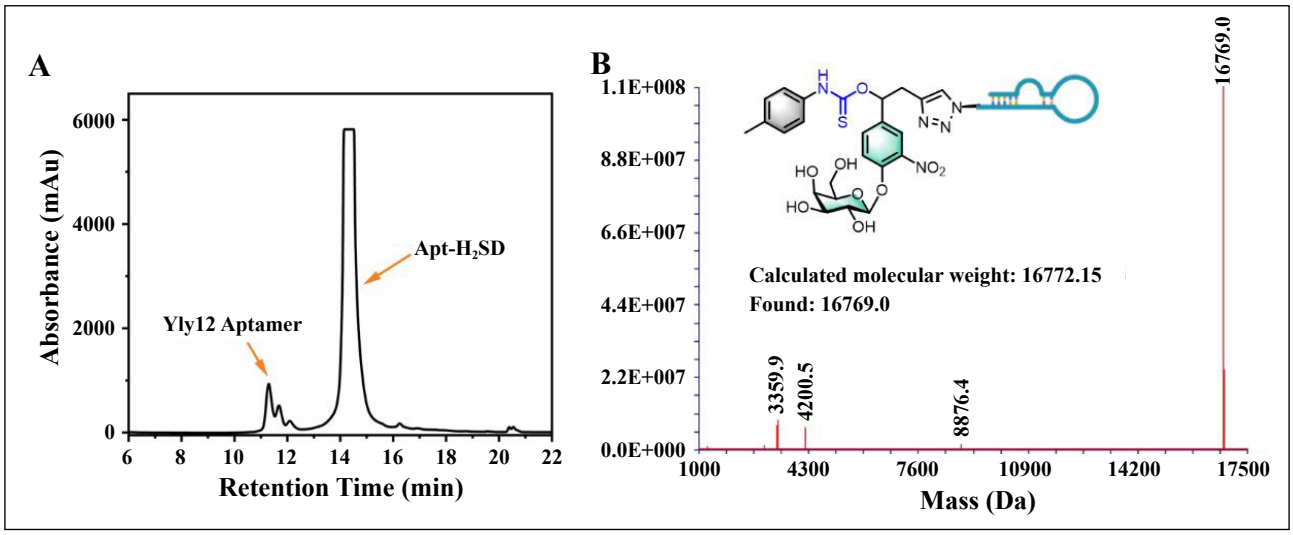

Figure S9. (**A**) HPLC purification profile of Apt-H_2SD. (**B**) ESI-MS spectrum of Apt-H_2SD**.**

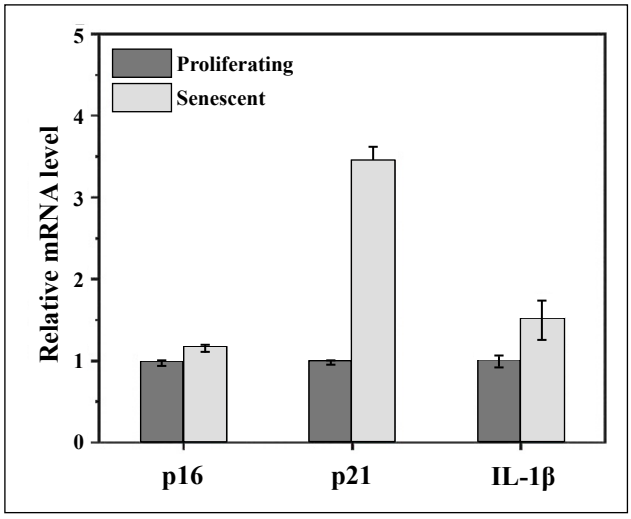

Figure S10. RT-qPCR qualification of the expression of p16, p21, and IL-1β at the mRNA level in proliferating BJ cells and senescent BJ cells.

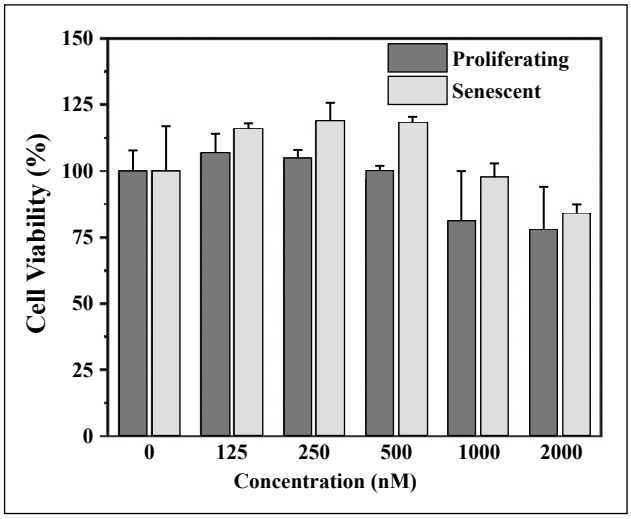

Figure S11. Cell viability of proliferating and senescent BJ cells after treatment with Apt-H_2SD at different concentrations.